On-orbit calibration of spaceborne microwave radiometer by using stable surface target

YANG Hu, YOU Ran, LU Nai-meng, QIU Hong, SHI Chun-xiang

Key Lab of Radiometric Calibration and Validation for Environmental Satellites, China Meteorological Administration (*LRCVES/CMA*) *and National Satellite Meteorological Center. Beijing* 100081, *China*

Abstract: Accurate calibration is needed for Quantitative application of space-borne passive microwave radiometers. In this paper, the surface target which can be taken as the calibration reference target are studied, and the emission model was developed for the emissivity computation for these targets. It is found that in dense covered forest area, for 19-89GHz frequencies, microwave radiation brightness temperature can be calculated with an accuracy of 1K. For the frequency channel as low as 6 and 10 GHz, the desert area such as sahara can be taken as reference calibration target. And the established model accuracy in desert area is within 2K by using the NCEP reanalysis dataset as input.

Key words: microwave radiometer, calibration model, ground target

CLC number: TP732.1 **Document code:** A

1 INTRODUCTION

Accurate calibration is needed for Quantitative application of space-borne passive microwave radiometer. Accurate calibration of a radiometer can be done by two methods: one is to carry out two-point calibration by using on-orbit blackbody and cold sky observation, which is the major on-orbit calibration method used for a space-borne microwave radiometer Tatnall & Jarrett, 1997 The advantage of this method is that calibration can be performed for each scan line. Since the accuracy of on-orbit two-point calibration can be affected by instrument gain drift and the radiation entered from the antenna side-lobe, the on-orbit cross-calibration of microwave radiometer by using the stable ground targets become a very important way for the accuracy validation of radiometer calibration accuracy (EOS technique report, 2002; Wentz *et al*., 1997; Hollinger *et al*., 1990).

Cross calibration by using ground targets requires the selection of two kinds of targets on the earth surface: targets with higher brightness temperature, like forest and desert, and those with lower- temperature microwave target like ocean surface. For previous one, tropical jungle and desert are most often used as calibration target, and the cross-calibration can be carried out in two stages (ESTEC technique report, 2004):

(1) Ground area is selected by using existing passive microwave radiometer data, the surface characteristics in these areas can be get from radiative transfer model simulation, and a specific model can be developed for the computation of surface emissivity in the selected area;

(2) In the on-orbit operating stage, the surface brightness temperature can be calculated by using the model derived in the first stage, and the value can be compared to the satellite observations, the correction for satellite measurements can be performed according to the comparison results.

In this paper, surface emissivity models for frequency from 6 to 89GHz in Amazon forest and Sahara Desert area are derived by using SSM/I data and numerical weather forecast analysis field NCEP data, the model accuracy are also evaluated.

2 EMISSIVITY MODEL FOR FOREST AREA

The model selected for clear-sky atmosphere absorption is Liebe atmospheric absorption model (Liebe *et al*., 1989, 1993). Liebe model requires atmospheric temperature and humidity profiles as model inputs. For the selected calibration area, the data sources for obtaining these parameters include radiosonde data and data from numerical weather forecast model(NCEP and ECMWF). Surface microwave radiation in dense vegetation covered area can be expressed by the following formula , without consideration of vegetation scattering (Brown & Ruf, 2005):

$$T_{\mathrm{Bcanopy}}(f,\theta,p)=\left(1+\frac{\Gamma_{\mathrm{s}}(f,\theta,p)}{L(f,\theta)}\right)\left(1-\frac{1}{L(f,\theta)}\right)\times [(1-\alpha(f)]T_{\mathrm{v}}+\left(1-\frac{\Gamma_{\mathrm{s}}(f,\theta,p)}{L(f,\theta)}\right)T_{\mathrm{s}} \quad (1)$$

Received: 2007-10-29; **Accepted**: 2008-01-22

Foundation: China National Science Foundation (No. 40601061).

First author biography: YANG Hu (1976—), received the Ph.D degree from the Institute of Remote Sensing Applications, Chinese Academy of Sciences, Beijing, in 2003. His main study interest includes passive microwave radiometer calibration, geophysical parameters retrieval and spaceborne active/passive instrument observation simulation.

where θ denotes ground incidence angle, f is observation frequency, p is polarization state, $\Gamma(f, \theta, p)$ is emissivity of interaction between soil and vegetation layer, $L(f, \theta)$ is vegetation layer attenuation factor, $\alpha(f)$ is single scattering albedo of vegetation layer, T_v is physical temperature of vegetation layer and T_s physical temperature of underlying surface. In the area with dense vegetation coverage, when frequency is larger than 10GHz, the attenuation factor of vegetation layer is very big and the transmittance is almost 0. Then except for direct radiation of vegetation layer, the main contribution of other items in Eq.(1) can be ignored. Under these circumstances, Eq.(1) can be simplified into

$$T_{\mathrm{Bcanopy}}(f) = (1-\alpha(f))T_{\mathrm{v}} \tag{2}$$

According to Eq.(2), microwave brightness temperature from vegetation layer is only relates to frequency and physical temperature. Therefore if atmospheric condition is known, microwave radiative brightness temperature of vegetation layer can be obtained through accurate computation by the radiative transfer model expressed by the following formula (Brown & Ruf, 2005):

$$T_{\mathrm{B}}(f,\theta) = (1-\alpha(f))T_{\mathrm{v}}\mathrm{e}^{-\tau(f)\sec\theta} + T_{\mathrm{B}}^{\mathrm{up}}(f,\theta) + \frac{\alpha(f)}{2}\times\left[\frac{1}{2\pi}\int_{2\pi} T_{\mathrm{B}}^{\mathrm{DN}}(f,\Omega')\cos\theta'\mathrm{d}\Omega'\right]\mathrm{e}^{-\tau(f)\sec\theta} \tag{3}$$

where $T_{\mathrm{B}}^{\mathrm{up}}$ stands for upward atmosphere radiative brightness temperature while $T_{\mathrm{B}}^{\mathrm{DN}}$ stands for downward atmosphere radiative brightness temperature. The first item in the right of the formula denotes the surface radiation through atmospheric attenuation, the second stands for the upward atmospheric radiation and the third is the downward atmosphere radiation reflected by the surface and accepted by the sensor through the atmospheric attenuation.

Calculation of microwave brightness temperature of dense vegetation layer by Eq.(3) requires determination of single scattering albedo $\alpha(f)$. Brown & Ruf (2005) found that in 18—40GHz fequencies, $\alpha(f)$ shows linear correlation with frequency, and in their study, a linear model was developed and used for calculation of 19—36GHz microwave brightness temperature in Amazon area. Results show that the model computation results is quite consistent with SSM/I observations. In Ruf's study, there is no considering for 85GHz channel. In our study, through RTM model simulation it is found that in 18—40GHz frequencies, showed positive correlation with frequency, which is in agreement with the previous study; for frequency higher than 40GHz, the single scattering albedo is decrease with increased frequency. As a result, in Amazon area, the Eq.(3) can be modified as a non-linear model, and therefore $\alpha(f)$ can be expressed as a secondary function of frequency:

$$\alpha(f) = a_0 + a_1 f + a_2 f^2 \tag{4}$$

After determination of T_v, atmospheric radiative brightness temperature and transmittance parameters, $\alpha(f)$ expressed in Eq.(4) is inserted into Eq.(3). Parameter ai in Eq.(4) is derived from multivariable regression model of Levenberg-Marquart iteration algorithm, which can be expressed as following:

$$\min\sum_{j=1}^{4}[f(T_{\mathrm{v}},a_0,a_1,a_2) - y^{(j)}]^2 \tag{5}$$

where f stands for the equation expressed in Eq.(3) for computation of brightness temperature radiative transfer, $y^{(j)}$ observational brightness temperature of 19—85GHz SSM/I. The parameter a derived from regression model is shown in Table 1. And the model computation error is showed in Table 2.

Table 1 Value of parameter a derived from regression model

Parameter	a_0	a_1	a_2
Regression value	0.0095926	0.0018535	−1.7589e 005

Table 2 Statistical comparison of model computed brightness temperature and SSM/I observation in 10—89 frequencies

Frequency /GHz	SSM/I observation/K	Model computed value	Mean deviation/K	RMS error/K
19	284.3±1	284.7	–0.4	0.08
23	283.5±1	283.0	0.5	0.08
36	280.1±1	280.3	0.2	0.08
85	284.2±1	284.3	0.1	0.1

3 EMISSIVITY MODEL FOR DESERT AREA

For bare surface as Sahara Desert, microwave radiative brightness temperature can be expressed by the following formula:

$$T_{\mathrm{B}}(f,\theta) = (1-R_{\mathrm{p}}^{\mathrm{e}})\cdot T_{\mathrm{eff}}\mathrm{e}^{-\tau(f)\sec\theta} + T_{\mathrm{B}}^{\mathrm{up}} + R_{\mathrm{p}}^{\mathrm{e}}\cdot T_{\mathrm{B}}^{\mathrm{DN}}\cdot\mathrm{e}^{-\tau(f)\sec\theta} \tag{6}$$

where T_{eff} stands for surface temperature, $R_{\mathrm{p}}^{\mathrm{e}}$ effective surface emissivity, $\tau(f)$ optical thickness and θ incidence angle of ground. In this project we employed a parameter model for calculation of effective surface emissivity (Shi *et al*., 2005). This model is derived from high-accuracy radiation transfer model for bare surface and expressed as follows:

$$R_{\mathrm{p}}^{\mathrm{e}} = Q_{\mathrm{p}}(f)\cdot r_{\mathrm{q}} + (1-Q_{\mathrm{p}}(f))\cdot r_{\mathrm{p}} \tag{7}$$

where Q_p is roughness parameter of surface in p-polarization status and a function of observation frequency f; R_p is Fresnel reflection factor and a function of surface dielectric constant and incidence angle. Thus we can parameterize Q_p from the observational brightness temperature value by microwave radiometer with known calibration accuracy and surface value to obtain an empirical expression of $Q_p(f)$. Then in actual calibration the top-of-atmosphere radiation brightness temperature in the interesting frequencies and observation area of incidence angle can be obtained in condition of Q_p parameters and measured surface parameters (surface temperature and soil moisture)

as well as atmospheric profiles data are known.

After the surface parameters (physical temperature and soil moisture), and atmospheric radiation contribution are known, the surface effective reflectivity can be determined from Eq.(5), and then $Q(f)$ term can be determined from Eq.(6), by regression analysis, the relationship between Q and frequencies can be expressed by the following formula:

$$Q(f) = a_1 \cdot f^{a_2} \tag{8}$$

where, a_1 and a_2 are model parameters and f observed frequency.

Parameter a_i in Eq.(8) is derived from multivariable regression model of Levenberg-Marquart iteration algorithm, and are shown in Table 3. The model error is shown in Table 4.

Table 3 Parameters value derived from regression model

Parameter	a_1	a_2
V-polarization	–0.1774	–1.0413
H-polarization	0.2277	0.1375

Table 4 Statistical comparison of model computed brightness temperature and SSM/I observation in 6 and 10Ghz frequencies in Sahara area

	Mean deviation	Standard deviation
6H	1.26	0.16
6V	1.31	0.20
10H	0.85	0.16
10V	1.31	0.16

It is clear from the statistical results that for V-pol and H-pol, the mean deviation of top-of-atmosphere brightness temperature and observed brightness temperature in 6GHz and 10GHz frequencies computed by model are both within 2K. In this study, model parameters are obtained by matching descending data with NCEP UTC00 grid data in the calibration area and by regression using 2m above air temperature as surface temperature. As AMSR-E descending-orbit data go through the Equator at 1:30 (local time), which corresponds to the universal time of 23:30 in the Sahara calibration area chosen. Mismatching of observed data with NCEP data in time will result in some error, which is also one of the sources of model computed errors. Moreover, The effective surface temperature is different from the air temperature 2m above surface due to surface thermal capacity, which also affects model computation accuracy.

4 ANALYSIS AND CONCLUSION

In this study, the surface emissive characteristics in Amazon forest and Sahara desert were studied for 19—89GHz channels by using DMSPF13-SSM/I data and NCEP data. For future on-orbit space-borne microwave radiometer calibration, these two area can be used as the reference ground target, and the following conclusions can be derived according to the study results:

1) In 19—40GHz frequencies the single scattering albedo in dense covered forest area is positively related to frequency. When observational frequency is greater than 40GHz, the single scattering albedo will decrease and emission of vegetation layer will increase. The relationship between scattering albedo and frequency can be modeled as a non-linear equation;

2) Analysis of the time series variation in surface 0cm temperature and brightness temperature has found that the time series variation of both is in good agreement and 0cm surface temperature in NCEP may be regarded as physical temperature of the vegetation layer for computation of brightness temperature;

3) In this study it is assumed that there is no polarization characteristic in the Amazon area. In fact V- and H-polarization difference <1K still occurs on the surface of the study area, which will introduce some error to the model accuracy.

Acknowledgements: The SSM/I data were kindly offered by NSIDC.

REFERENCES

Brown S T and Ruf C S. 2005. Determination of an amazon hot reference target for the on-orbit calibration of microwave radiometers. *Journal of Atmospheric and Oceanic Technology*, **22**: 1340—1352

EOS technique report. 2002. AMSR/AMSR-E Calibration and Validation Plan. Earth Observation Research Center

ESTEC technique report. 2004. Final Report:Passive Calibration of the Backscattering Coefficient of the Envisat RA-2. N.15925/02/NL/SF

Hollinger J P, Peirce J L and Poe G A. 1990. SSM/I instrument evaluation. *IEEE Transactions on Geoscience and Remote Sensing*, **28**(5): 781—790

Liebe H J, Hufford G A and Cotton M G. 1993. Propagation modeling of moist air and suspended water/ice particles below 1000GHz. AGARD Fifty-second Special Meeting of the panel on Electromagnetic wave propagation. Advis. Group Aerosp. Res. Dev. Palma De Malorca, Spain

Liebe H J. 1989. MPM-An Atmospheric millimeter-wave propagation model. *International Journal of Infrared and Millimeter Waves*, **10**(6): 631—649

Shi J, Jiang L M, Zhang L X, Chen K S, Wigneron J P and Chanzy A. 2005. A parameterized multi-frequency-polarization surface emission model. *IEEE Transactions on Geoscience and Remote Sensing*, **43**(12): 2831—2841

Tatnall A R L. and Jarrett M L. 1997. The calibration of passive microwave sensors. *Adv.Space Res.*, **19**(9): 1409—1414

Wentz F, Ashcroft P, Gentemann C. 1997. Post-Launch calibration of the TRMM microwave imager. RSS technique report

星载微波辐射计交叉定标中陆面目标辐射亮温计算模型

杨 虎, 游 然, 卢乃锰, 邱 红, 师春香

中国气象局 中国遥感卫星辐射测量和定标重点开放实验室, 国家卫星气象中心, 北京 100081

摘 要: 从被动微波辐射计在轨辐射定标的角度出发, 选取亚马逊雨林作为高温地面目标, 利用 DMSPF13-SSM/I 数据和 NCEP 数据对研究区 19—89GHz 辐射特性进行分析。研究发现, 利用辐射亮温稳定的热带雨林作为地面目标, 对 19—89GHz 的频段, 微波辐射亮温计算精度可以达到 1K 以内; 对于 6 和 10GHz 这样的低频通道, 撒哈拉沙漠是一个可供选择的地面目标, 根据所建立的亮温计算模型, 利用数值预报分析场 NCEP 数据作为输入, 其亮温计算精度在 2K 以内。

关键词: 微波辐射计, 定标, 辐射量温计算模型

中图分类号: TP732.1 文献标识码: A

1 引 言

星载被动微波辐射计定量应用需要对仪器进行精确标定。辐射计定标可以通过 2 种方法实现: 一是利用星上黑体和冷空观测进行两点定标, 这种方法的优点是每条扫描线可以得到定标观测数据, 定标频次和定标精度较高, 这是微波辐射计在轨定标的主要手段(Tatnall & Jarrett, 1997)。由于仪器增益漂移以及冷空观测当中旁瓣的影响, 星上两点定标精度会受到影响。利用地面辐射亮温稳定的目标进行微波辐射计定标是微波辐射计在轨辐射定标的一个重要补充手段(EOS technique report, 2002; Wentz 等, 1997; Hollinger 等, 1990)。

利用地面目标进行辐射计标定需要在地表选取 2 种目标: 高温微波辐射目标和低温微波辐射目标。高温目标一般选取热带雨林和沙漠; 低温目标一般选取稳定的海表。利用地表目标进行交叉定标分为 2 个阶段进行(ESTEC technique report, 2004):

(1) 用已有的被动微波辐射计数据作为模拟数据, 选取定标训练区域, 针对这些区域地表特性建立用于微波亮温模拟计算的辐射传输模型, 并对模型精度和敏感性进行验证;

(2) 在辐射计在轨运行阶段, 针对在轨辐射计在定标测试区域实际获取的数据, 用第一阶段建立的模型计算辐射计感兴趣频段地表微波辐射亮温, 完成定标过程。

以往研究工作表明, 雨林、沙漠、稳定的海表可以作为地面定标目标对辐射计进行标定(Wentz 等, 1997)。亚马逊雨林、撒哈拉沙漠、以及中国云南地区存在微波辐射亮温稳定的区域。在这些区域, 针对不同微波频率和极化通道, 建立满足精度要求的目标辐射亮温计算模型是替代定标的一个重要研究内容。本研究以亚马逊雨林和撒哈拉沙漠为例, 利用星载微波辐射计 SSM/I 数据和数值天气预报分析场 NCEP 数据, 针对 6—89GHz 频段 V 和 H 极化通道分别建立了目标场辐射亮温计算模型, 并对模型精度进行了评价。

2 方 法

微波亮温计算模型选取主要研究内容是针对选定的定标区域, 收集在仪器定标期间实际可用的不同来源的数据, 并把这些数据通过统一的接口输入到地表亮温计算模型中。具体数据处理流程见图 1。

收稿日期: 2007-10-29; 修订日期: 2008-01-22

基金项目: 国家自然科学基金(编号: 40601061)。

第一作者简介: 杨虎(1976—), 男, 中国科学院遥感应用研究所理学博士, 副研究员。目前主要研究方向微波辐射定标, 主被动微波数据处理和地表参数反演, 已发表论文 10 篇。

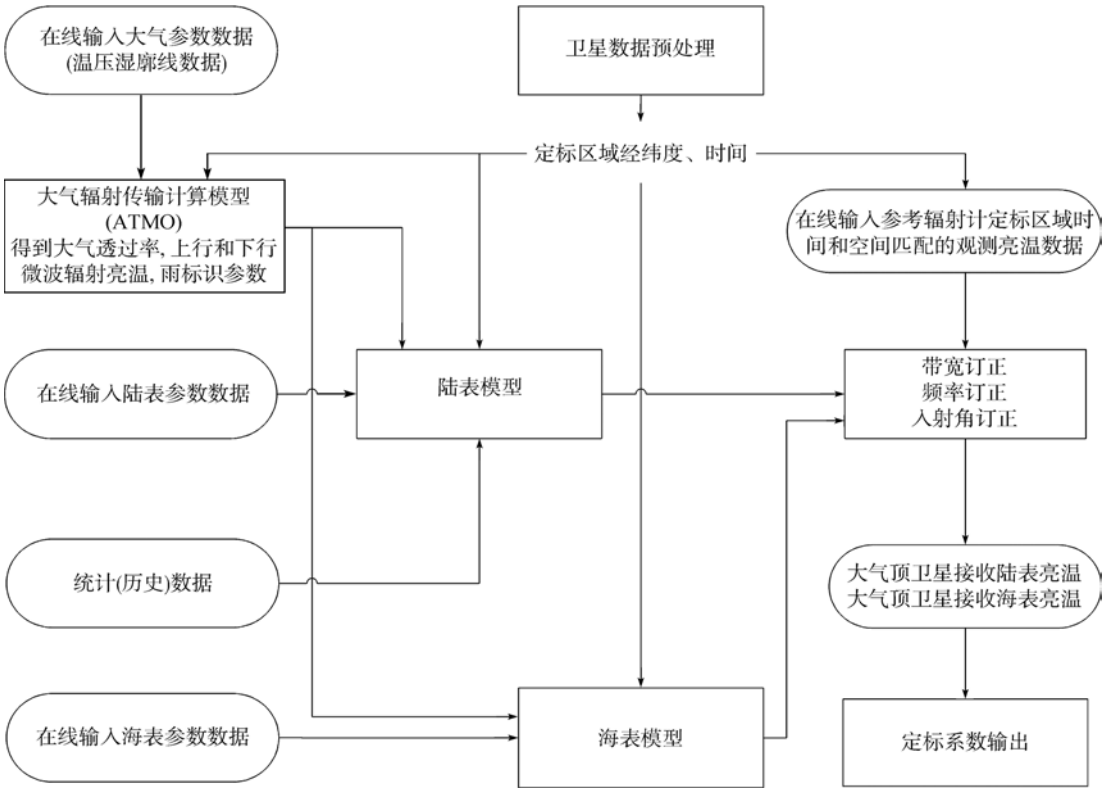

图 1　交叉定标流程

2.1　大气模型建立及输入数据选取

被动定标中晴空大气条件下亮温计算选择的模型为 Liebe 大气吸收模型(Liebe 等, 1989, 1993)。Liebe 模型要求有大气温度、湿度、气压剖面作为输入参数, 模型的精度取决于这些输入参数数据的测量精度。对于选定的定标区域, 获取这些参数可供选择的数据源有常规探空数据和数值天气预报中心(NCEP 和 ECMWF)的分析场数据。

2.2　致密植被覆盖地表微波辐射亮温计算模型的建立

研究中选取亚马逊雨林作为陆表高温目标进行定标研究。选取亚马逊雨林作为微波辐射计定标区域有以下几点考虑:

(1) 目标区域覆盖范围的考虑。考虑到辐射计天线波束宽度、扫描几何、地球覆盖等因素, 要求定标区有足够大的范围, 以使定标区域能够覆盖几个天线波束视场, 在定标区域得到足够亮温观测数据, 从而能够从这些观测数据进行平均, 得到有效目标辐射亮温。

(2) 目标区域温度均匀性考虑。类似于星上黑体, 选取的地面目标必须是一个温度均匀性程度较高的区域, 其温度梯度不能过大, 否则无法得到有效目标辐射亮温。

(3) 目标发射率稳定性考虑。选取的目标在测试频段的微波发射率必须是稳定的, 即目标发射率只与测试辐射计频率相关, 不随时间变化而变化, 这样才能够由微波辐射传输模型从目标发射率和目标物理温度计算出目标真实辐射亮温。

不考虑植被散射, 植被覆盖地表微波辐射可用下式表示(Brown & Ruf, 2005):

$$T_{\mathrm{Bcanopy}}(f,\theta,p)=\left(1+\frac{\Gamma_{\mathrm{s}}(f,\theta,p)}{L(f,\theta)}\right)\left(1-\frac{1}{L(f,\theta)}\right)\times [(1-\alpha(f)]T_{\mathrm{v}}+\left(1-\frac{\Gamma_{\mathrm{s}}(f,\theta,p)}{L(f,\theta)}\right)T_{\mathrm{s}} \tag{1}$$

上式, θ为地面入射角, f 为观测频率, p 为极化状态, $\Gamma(f, \theta, p)$为土壤-植被层相互作用的反射率, $L(f, \theta)$为植被层衰减因子, $\alpha(f)$为植被层单散射反照率, T_{v} 为植被层物理温度, T_{s} 为下垫面物理温度。在致密植被覆盖区域, 当频率>10GHz 时, 植被层衰减因子很大, 透过率几乎为 0, 这时除植被层直接辐射外, 式(1)中其余项的贡献可以忽略不计。这种情况下, 式(1)可以简化为:

$$T_{\mathrm{Bcanopy}}(f)=(1-\alpha(f))T_{\mathrm{v}} \tag{2}$$

根据式(2), 植被层微波辐射亮温只与频率和物理温度相关。这样, 如果大气状况已知, 则植被层微波辐射亮温可以通过下式表示的辐射传输模型准确计算

得到(Brown & Ruf, 2005):

$$T_{\mathrm{B}}(f,\theta)=(1-\alpha(f))T_{\mathrm{v}}\mathrm{e}^{-\tau(f)\sec\theta}+T_{\mathrm{B}}^{\mathrm{up}}(f,\theta)+\frac{\alpha(f)}{2}\times\left[\frac{1}{2\pi}\int_{2\pi}T_{\mathrm{B}}^{\mathrm{DN}}(f,\Omega')\cos\theta'\mathrm{d}\Omega'\right]\mathrm{e}^{-\tau(f)\sec\theta} \tag{3}$$

上式，$T_{\mathrm{B}}^{\mathrm{up}}$ 表示大气上行辐射亮温；$T_{\mathrm{B}}^{\mathrm{DN}}$ 表示大气下行辐射亮温。公式右边第一项表示经过大气衰减的地表辐射量，第二项表示大气上行辐射，第三项表示大气下行微波辐射被地表反射部分经过大气衰减被传感器接收部分。

用式(3)计算致密植被层微波辐射亮温，需要确定单散射反照率$\alpha(f)$。Ruf 等人通过理论模型模拟和机载辐射计观测发现，在 18—40GHz 频率范围，$\alpha(f)$与频率呈线性正相关，并且用这样一个线性模型对亚马逊雨林 19—36GHz 微波辐射亮温进行计算，得到与 SSM/I 观测亮温非常一致的结果(Brown & Ruf, 2005)。但是 Ruf 的研究当中没有对 85GHz 给出亮温计算模型。在对亚马逊雨林的研究中，通过理论模型模拟和实际卫星观测亮温分析发现，在 18—40GHz，$\alpha(f)$与频率成正相关，这与前人的研究结果一致；而当频率高于 40GHz 时，植被层辐射率有增高的现象，可能的解释是，当频率>40GHz 时，植被反射大气向下辐射亮温增强。这样，在应用式(3)对亚马逊雨林微波辐射亮温计算时，$\alpha(f)$的计算采用一个频率的二次函数来表示:

$$\alpha(f)=a_0+a_1f+a_2f^2 \tag{4}$$

2.3 裸露地表微波辐射亮温计算模型的建立

对撒哈拉沙漠这样的裸露地表，微波辐射亮温可以用下式表示:

$$T_{\mathrm{B}}(f,\theta)=(1-R_{\mathrm{p}}^{\mathrm{e}})T_{\mathrm{eff}}\mathrm{e}^{-\tau(f)\sec\theta}+T_{\mathrm{B}}^{\mathrm{up}}+R_{\mathrm{p}}^{\mathrm{e}}T_{\mathrm{B}}^{\mathrm{DN}}\mathrm{e}^{-\tau(f)\sec\theta} \tag{5}$$

上式，T_{eff}为地表温度，$R_{\mathrm{p}}^{\mathrm{e}}$为地表有效发射率，$\tau(f)$为光学厚度，$\theta$为地面入射角。

本研究中，采用一个参数化模型进行地表有效发射率计算(Shi 等，2005)。该模型基于高精度裸露地表辐射传输模型发展而来，表示如下:

$$R_{\mathrm{p}}^{\mathrm{e}}=Q_{\mathrm{p}}(f)r_{\mathrm{q}}+(1-Q_{\mathrm{p}}(f))r_{\mathrm{p}} \tag{6}$$

式中，Q_{p}为 p 极化状态地表粗糙度参数，是观测频率f的函数；R_{p}为 Fresnel 反射系数，是地表介电常数和入射角的函数。这样，如果能够从已知定标精度的微波辐射计观测亮温值和地表测量值的数据中对Q_{p}进行参数化，得到 $Q_{\mathrm{p}}(f)$的经验表达式，那么在实际定标中，就可以根据确定的Q_{p}参数和地表参数测量值(地表温度、土壤水分)，以及大气廓线数据，得到感兴趣的频段和入射角观测区大气顶辐射亮温。

3 亚马逊雨林微波辐射亮温计算

3.1 数据源

亮温数据选取 DMSPF13-SSM/I 25km 分辨率全球 EASE-GRID 投影亮温数据。DMSPF13 升轨道地方时为 18: 33；降轨道地方时为 06:33。同时选取时间匹配的 NCEP 再分析场数据中地表 0cm 温度作为植被层物理温度，同时用其中的大气廓线数据作为微波晴空大气辐射亮温计算的输入。

3.2 研究区域选取

亚马逊雨林地区除致密植被覆盖区域外，还有河流和水系。当辐射计视场中有水体存在时，会严重影响辐射计观测亮温，使亮温降低。由上面的分析知道，在微波频段，极化的产生主要由于地表微波辐射的作用，在致密植被覆盖区域，微波辐射是各向同性的，且没有极化差。为使式(2)成立，必须选取窗区通道亮温极化差很小的像元。根据 Ruf 等的研究结果(Brown & Ruf, 2005)，我们用 SSM/I19 GHz 和 37GHz 通道 V 和 H 极化亮温差做为区域选取判据，选取的区域满足如下条件:

均值 Mean(BT19v-BT19h) < 0.75K；方差 std (BT19v-BT19h)<0.80K;

均值 Mean(BT19v-BT19h) < 0.75K；方差 std (BT19v-BT19h)<0.78K;

根据这一判据选取的亚马逊雨林定标区域范围有两个:

区域 A：纬度范围为：4°N—1°S；经度范围为：53°W—59°W;

区域 B：纬度范围为：5°S—10°S；经度范围为：65°W—74°W;

本研究用区域 A 的观测数据建立亮温计算模型。剔除降水的影响，对选取的区域的微波辐射亮温做日平均，得到与 NCEP 数据匹配的 2004 年全年共 196 个数据。利用这些数据作为定标分析。区域 B 的观测数据用来做模型验证。

3.3 辐射亮温计算

3.3.1 大气微波辐射亮温计算

要从式(3)中计算得到定标区域辐射亮温，首先进行研究频段(19—85GHz)大气上行和下行微波辐射亮温计算，以及不同频段大气光学厚度和透过率计算。图 2 为利用 NCEP 数据计算的研究区域 19—

85GHz 大气上行和下行辐射亮温。

3.3.2　植被层物理温度数据分析

研究中，假定 NCEP 数据中的 0cm 地表温度(LST_0)为植被层物理温度(T_v)，将其带入式(3)进行计算。为验证这种假定的合理性，我们同时将 LST_0 和不同频率观测亮温的时间序列变化比较。图 3 是比较结果。

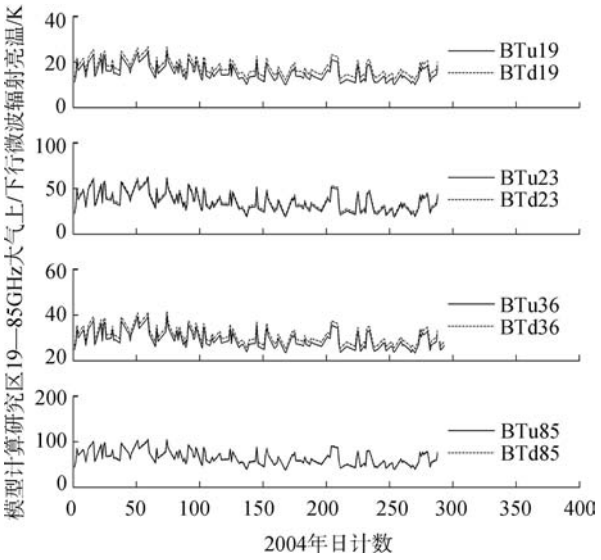

图 2　利用 NCEP 数据计算的区域 A 19—89GHz 大气上行和下行微波辐射亮温

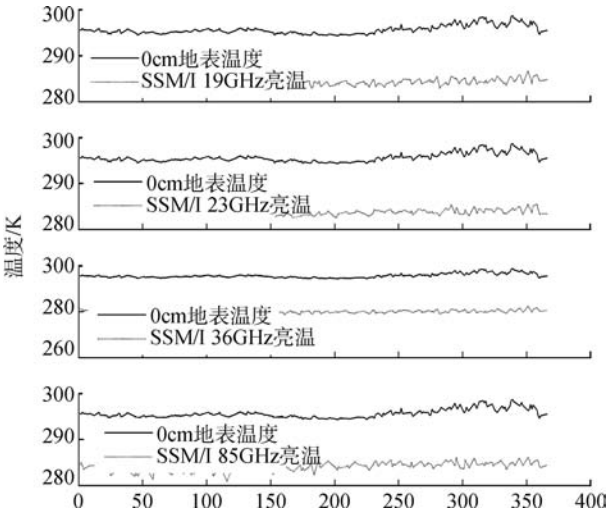

图 3　LST_0 和 BT 的时间序列变化比较

图 3 中 LST_0 数据由 NCEP 数据中得到的本地时间 03 点数据，SSM/I 亮温数据为本地时间 06:33 数据，由于是在日出前，所以时间上可以认为是匹配的。结果表明，在 19—85GHz 的所有频率点，SSM/I 观测研究区微波辐射亮温的时间序列变化趋势与 LST_0 的时间序列趋势非常吻合。由此我们可以得到如下两点结论:

(1) 将 LST_0 作为植被层物理温度 T_v 的假设是合理的;

(2) 研究区域地表发射率随时间变化不大，可以认为是稳定的。

3.3.3　研究区植被层单散射反照率的确定

确定了 T_v 和大气辐射亮温和透过率参数，将式(4)表示的 $\alpha(f)$ 带入式(3)，用多变量回归的 Levenberg-Marquart 迭代算法回归得到式(4)中的系数 a_i, i=0,2。

算法表达式如下:

$$\min \sum_{j=1}^{4} [f(T_v, a_0, a_1, a_2) - y^{(j)}]^2 \qquad (7)$$

式中，f 为式(3)表达的亮温辐射传输计算方程，$y^{(j)}$为 19—85GHz SSM/I 观测亮温。回归得到的系数 a 如表 1。

表 1　回归得到的系数 a 的值

系数	a_0	a_1	a_2
回归值	0.0095926	0.0018535	−1.7589e 005

3.3.4　定标区 **19—89GHz** 频段亮温计算结果

将回归得到的系数 a 带入式(4)，利用式(3)计算得到区域 B 19—85GHz 频率微波辐射亮温。图 4 给出了式(3)计算值与 SSM/I 实际观测亮温的比较结果(表 2)。

表 2　模型计算结果与实际 **SSM/I** 观测亮温值的比较

频率/GHz	SSM/I 观测值/K	模型计算值	平均偏差/K	均方根误差/K
19	284.3±1	284.7	−0.4	0.08
23	283.5±1	283.0	0.5	0.08
36	280.1±1	280.3	0.2	0.08
85	284.2±1	284.3	0.1	0.1

4　撒哈拉沙漠地表亮温计算

模型分析和实际测量亮温数据表明，在 6GHz 和 10GHz 频段，微波对亚马逊雨林这样的致密植被覆盖区域仍然具有一定的穿透性。这样，地表的变化会在一定程度上影响到场区微波发射率的稳定性和均匀性，使得上节设定的致密植被辐射亮温模型不成立。所以，亚马逊雨林只能用于 10GHz 以上频率辐射计的标定。对低频，我们用撒哈拉沙漠进行亮温标定。

4.1 定标区域选取和数据处理

定标区域选取亮温分布比较均匀的区域，以6GHz和10GHz H极化通道亮温标准差为均匀性判识因子，在撒哈拉沙漠选取亮温标准差小于1K的区域作为定标区域，选取2个满足条件的区域:

区域A, N18.99°—N21°,W9.37°—W6.77°;

区域B: N15.11°—N18.37°; E11.71°—E15.88°;

把区域A作为定标数据训练区域，用于发展模型参数；区域B作为定标精度验证区域，用于模型验证。

亮温数据采用2004年1—10月AMSR-E L2A降轨道数据，大气和地表参数数据使用研究区NCEP UTC00点数据。图5分别是AMSR-E 6-18GHz V极化亮温和H极化亮温与NCEP 2m高度地温日变化趋势的比较。可以看出，2m高度气温和微波辐射亮温日变化之间有很好的相关性，所以研究中，利用式(5)计算辐射亮温时，地表温度取2m高度气温。

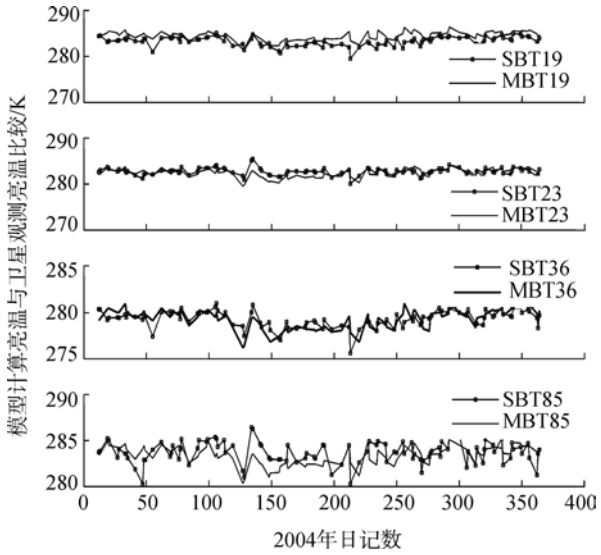

图4 模型计算区域B 10—85GHz亮温与SSM/I实际观测亮温的比较(SBT:SSM/I观测亮温, MBT:模型计算亮温)

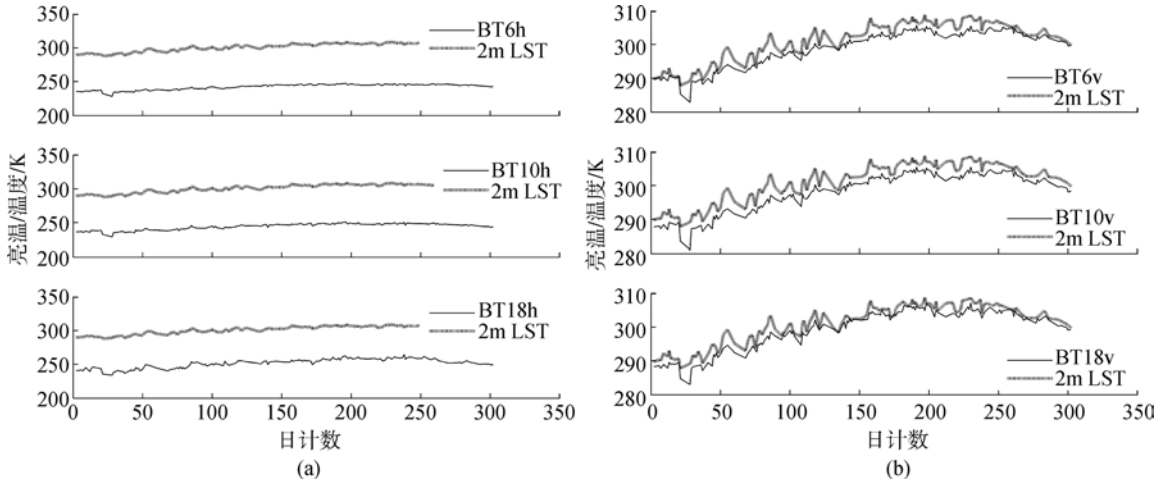

图5 AMSR-E 6-18GHz极化亮温和2m地温的日变化趋势

(a)H极化; (b)V极化

4.2 撒哈拉沙漠粗糙度参数的确定

确定了地表温度和大气辐射亮温和透过率参数，地表介电常数实部取4.06,虚部取0.30，将式(7)中的$Q(f)$用下式表示:

$$Q(f)=a_1 f^{a_2} \tag{8}$$

式中，a_1, a_2为模型系数，f为观测频率。

综合式(6)—式(8)，对区域A中的数据，用多变量回归的Levenberg-Marquart迭代算法回归得到式(8)中的系数a_i, i=1,2，如表3。

4.3 结果和分析

用区域B中的数据对模型进行验证，验证结果如图5和图6。

模型计算结果与卫星观测亮温的平均偏差和均方根误差如表4。

表3 回归得到的系数 a 的值

系数	a_1	a_2
V极化	−0.1774	−1.0413
H极化	0.2277	0.1375

表4 模型计算与卫星观测亮温的偏差和均方根误差

极化	偏差平均值	标准差
6H	1.26	0.16
6V	1.31	0.20
10H	0.85	0.16
10V	1.31	0.16

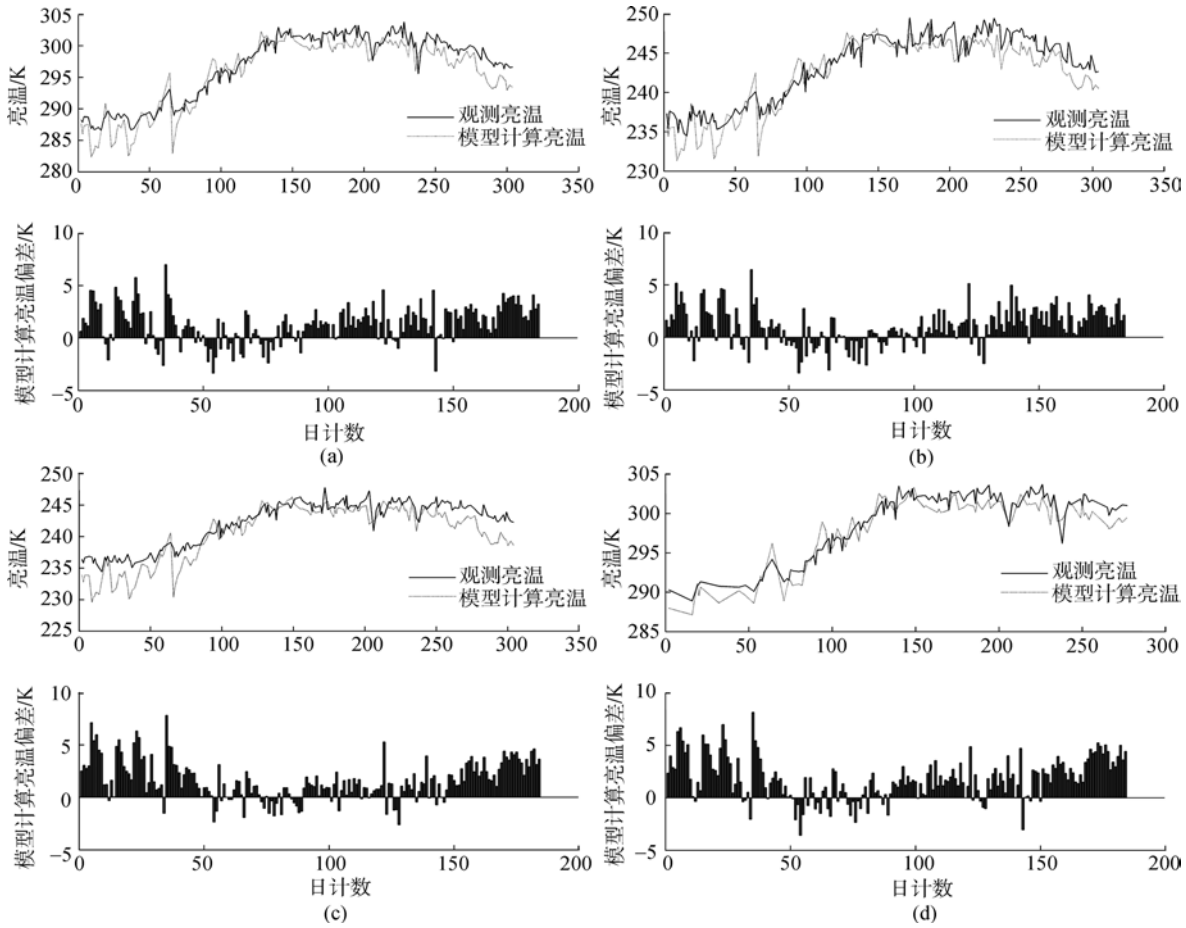

图 6　撒哈拉沙漠 6, 10GHz V 和 H 极化模型计算亮温与卫星观测亮温日变化比较
(a) 10GHz V 极化; (b) 10GHz H 极化; (c) 6GHz H 极化; (d) 6GHz V 极化

从统计结果看出，对 V 和 H 极化，模型计算得到 6GHz 和 10GHz 大气顶亮温与卫星观测亮温的平均偏差在 2K 以内。本研究中，我们用降轨数据和定标区 NCEP UTC00 点数据相匹配，并且用 2m 气温作为地表温度回归得到了模型系数。由于 AMSR-E 降轨数据过赤道时间为当地时间 1:30，对应于所选撒哈拉定标场区世界时 23:30。卫星观测数据与 NCEP 数据时间上的不匹配会带来一定误差，这是模型计算误差的来源之一。另一方面，用的数据为夜间数据，由于地表热容量的存在，实际地表温度和 2m 气温有一定差别，这也影响到模型计算精度。

5　分析和结论

本研究中，我们从被动微波辐射计在轨辐射定标的角度出发，选取亚马逊雨林作为高温地面目标，利用 DMSPF13-SSM/I 数据和 NCEP 数据对研究区 19—89GHz 辐射特性进行了分析。研究发现:

(1) 在 19—40GHz 频率范围，植被单散射反照率只与频率相关，且与频率成正相关；当观测频率高于 40GHz 时，单散射反照率下降，植被层辐射有增大的现象，由此发展了一个单散射反照率与频率的二次模型来表示这种特性，进一步由多变量最小二乘算法回归得到了模型系数;

(2) 分析地表 0cm 温度与亮温的时间序列变化发现，二者时间序列变化有很好的一致性，可以将 NCEP 中的 0cm 地表温度作为植被层物理温度进行亮温计算;

(3) 本研究中假定研究区微波辐射没有极化特性，实际上，研究区地表仍然存在<1K 的 V 和 H 极化差，这会对模型计算精度产生一定影响。

用本研究发展的模型算法对亚马逊雨林 19—89GHz 微波辐射亮温计算精度<1K。这个结果是以 SSM/I 定标精度为前提。本文用 DMSPF13 卫星进行了分析，由于 DMSPF13-F15 卫星过赤道时间从本地

时间06点到21:00，并且SSM/I传感器稳定，且星上定标精度<1K,下一步工作可以利用这些数据可以进一步发展出目标亮温随时间变化的辐射传输计算模型，由此可以对在这一时间段的测试辐射计进行定标，而不需要有与待测试辐射计时间匹配的 SSM/I 数据。

REFERENCES

Brown S T and Ruf C S. 2005. Determination of an amazon hot reference target for the on-orbit calibration of microwave radiometers. *Journal of Atmospheric and Oceanic Technology*, **22**: 1340—1352

EOS technique report. 2002. AMSR/AMSR-E Calibration and Validation Plan. Earth Observation Research Center

ESTEC technique report. 2004. Final Report:Passive Calibration of the Backscattering Coefficient of the Envisat RA-2. N.15925/02/NL/SF

Hollinger J P, Peirce J L and Poe G A. 1990. SSM/I instrument evaluation. *IEEE Transactions on Geoscience and Remote Sensing*, **28**(5): 781—790

Liebe H J, Hufford G A and Cotton M G. 1993. Propagation modeling of moist air and suspended water/ice particles below 1000GHz. AGARD Fifty-second Special Meeting of the panel on Electromagnetic wave propagation. Advis. Group Aerosp. Res. Dev. Palma De Malorca, Spain

Liebe H J. 1989. MPM-An Atmospheric millimeter-wave propagation model. *International Journal of Infrared and Millimeter Waves*, **10**(6): 631—649

Shi J, Jiang L M, Zhang L X, Chen K S, Wigneron J P and Chanzy A. 2005. A parameterized multi-frequency-polarization surface emission model. *IEEE Transactions on Geoscience and Remote Sensing*, **43**(12): 2831—2841

Tatnall A R L. and Jarrett M L. 1997. The calibration of passive microwave sensors. *Adv.Space Res.*, **19**(9): 1409—1414

Wentz F, Ashcroft P, Gentemann C. 1997. Post-Launch calibration of the TRMM microwave imager. RSS technique report